Trans. of the Society of Instrument and Control Engineers Vol. E-1, No.1 20/26 (2001)

A Magnetic Flowmeter with Conducting Pipe Wall

Hiro YAMASAKI*, Satoshi HONDA*, Dongzhi JIN* and Chuji AKIYAMA+

The internal pipe wall of magnetic flowmeters must have been non-conductive to prevent generated electromotive force from short-circuiting. Usually the inside of metallic pipe is lined with insulating material. The lining limits applicable temperature range of measured fluid and also its reliability. A new structure is proposed, in which the insulating liner is eliminated. A potential distribution is formed on the pipe wall by applying voltage proportional to fluid flowrate. The potential distribution is kept nearly identical to the flow-induced potential in the fluid so that no current flows across the boundary between fluid and the pipe wall. Therefore the output signal is exactly the same as that of conventional magnetic flowmeters. In this paper theoretical analysis and experimental results are described.

Key Words: magnetic flowmeters, process instrumentation, potential distribution, virtual insulation, flowrate sensor

1 Introduction

The magnetic flowmeter is widely used in process instrumentation as one of the major liquid flow metering devices. Its obstruction-less structure and linear flow characteristics are of great advantage in this field.

In some applications, however, a magnetic flowmeter cannot be used due to its poor corrosion-proof characteristics or the limited applicable temperature range of the insulating material used as inside wall liner. The insulating liner is necessary for detection of correct output signals because it prevents short-circuiting of the flow-induced electric field.

Abrasion of the insulating liner changes the diameter of the flow conduit, which may cause the error. The cost of the lining process in manufacturing may be another problem.

The objectives of this investigation are to develop a new magnetic flowmeter, which has metallic flow conduit without any insulating liner, and to expand the applicable area of magnetic flowmeters with improved reliability.

The principle of the proposed magnetic flowmeter is to realize an equivalent boundary condition between fluid and metallic pipe wall. A potential distribution is formed on the pipe wall by applying electric voltage proportional to fluid flowrate.

The potential distribution on the wall is kept nearly identical to the flow-induced potential in the fluid so that no current flows across the boundary between fluid and the pipe wall. Thus the boundary condition is kept equivalent to that of non-conducting pipe wall automatically by the use of electronic servo techniques. Therefore the output signal is exactly the same as that of conventional magnetic flowmeters.

The first report of our study was presented to SICE Annual Meeting in 1981[1]. In this paper, our theoretical analysis is summarized and test results by experimental model are described.

2 Principles

2.1 Principle of magnetic flowmeters

When a conductive material is moving with velocity $\boldsymbol{V}$ in a magnetic field $\boldsymbol{B}$, Maxwell's equations tell us an electric potential U is induced across the material as shown in equation (1):

$$\Delta U = \mathrm{div}(\boldsymbol{V} \times \boldsymbol{B}) = \boldsymbol{B}\ \mathrm{rot}\ \boldsymbol{V} - \boldsymbol{V}\ \mathrm{rot}\ \boldsymbol{B} \qquad (1)$$

Let us use Cartesian coordinate system X-Y-Z to describe the arrangement of the meter, as shown in **Fig. 1**.

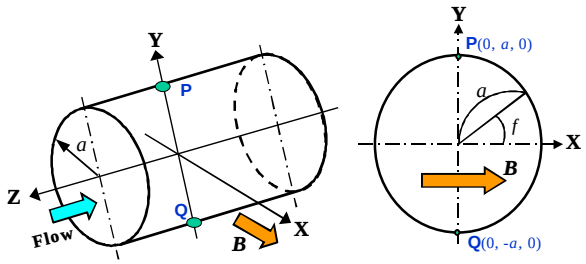

(a) Coordinate system of magnetic flowmeter having circular flow conduit

(b) Flow pipe electrodes and magnetic field

Fig. 1

The inner radius of flow conduit is denoted by a. We can assume that the flow velocity $\boldsymbol{V}$ has only one component V in the direction of the Z-axis, and the flow velocity profile being symmetrical to that axis. We can also assume that the magnetic flux density $\boldsymbol{B}$ is uniform, having a single component, B, in the direction of the X-axis.

A pair of potential-sensing electrodes are located at P(0, a, 0) and Q(0, $-a$, 0) on the Y-axis, as shown in **Fig. 1**. Then the problem can be reduced to a two-dimensional problem and can be reduced by utilizing a polar co-ordinate system using r and f. Then, the equation (1) can

* The University of Tokyo, Hongo, Bunkyo-ku, Tokyo, Japan
+ Yokogawa Electric Corp., Musashino, Tokyo, Japan

be simplified as equation (2):

$$\Delta U = B \frac{\partial V}{\partial y} \tag{2}$$

where U is the potential, V is the flow velocity vector, and B is the magnetic flux density.

2.2 Potential on the pipe wall and boundary conditions

(1) Non-conducting pipe wall

Let us discuss first, the case of a non-conducting pipe wall as conventional magnetic flowmeters.

The boundary condition of this case is given by equation (3), which is the boundary condition at the inner surface of insulating liner of the pipe.

$$\frac{\partial U}{\partial r} = 0, \quad \text{at } r = a \tag{3}$$

where $r = \sqrt{x^2 + y^2}$

The solution of equation (2) is given as (4) under the above boundary condition.

$$U(x,y) = Im\left\{\frac{B}{2p}\iint_D V(x,h)\left[\frac{1}{z-z} + \frac{a^2}{z^*(a^2 - zz^*)}\right]dxdh\right\} \tag{4}$$

where $z = e + ix$, $z^* = e - ix$, $z = x + iy$, and $Im(\bullet)$ denotes the imaginary part of a complex variable. Domain of a double integral D is the pipe cross section including the electrodes.

Now that we have an axially symmetrical flow velocity distribution, we can change coordinate system from the Cartesian (x, h) to the polar one (r, q).

Then $z = r e^{iq}$, $z = a e^{if}$

Since the flow is axially symmetrical,

$$V(r, q) = V(r)$$

Potential on the pipe wall boundary at $q = f$ is given by equation (5).

$$U(a, f) = Im\left\{\frac{B}{2p}\int_0^{f}\int_0^{a} V(r)\left[\frac{1}{r e^{iq} - a e^{if}} + \frac{a}{r e^{-iq}(a - r e^{if} e^{-iq})}\right] r\, dr dq\right\} \tag{5}$$

The result of the equation (5) is given as equation (6).

$$U(a, f) = B\, a\, \bar{\nabla} \sin f \tag{6}$$

where $\bar{\nabla}$ is the mean flow velocity given by equation (7):

$$\bar{\nabla} = \frac{1}{p a^2}\int_0^{a} V(r)\, 2pr\, dr \tag{7}$$

As the two electrodes, P and Q, are located at $(a, p/2)$ and $(a, -p/2)$, respectively, the potential difference $U_{f\,PQ}$ between the electrodes P and Q is obtained from equation (6), where f is substituted by $p/2$ at P, and by $-p/2$ at Q as shown in equation (8). Thus we get the well known magnetic flowmeter output voltage.

$$U_{f\,PQ} = U_{f\,P} - U_{f\,Q} = U(a, \frac{p}{2}) - U(a, -\frac{p}{2}) = 2Ba\bar{\nabla} \tag{8}$$

where $U_{f\,P}$ and $U_{f\,Q}$ are fluid potential at P and Q respectively.

Equation (6) indicates that the angular potential distribution on the wall is a sinusoidal function of f, where $\bar{\nabla}$ is the mean flow velocity.

(2) Conducting pipe wall

Next, let us discuss the case of the conducting pipe wall. Here the problem is, how the conductivity and the potential of the conducting pipe wall influence the flowmeter output.

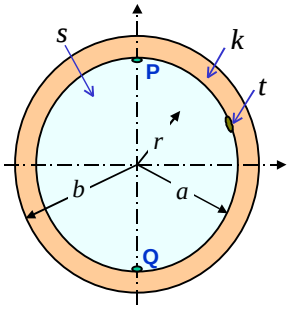

Fig. 2 Cross Section of conducting flow conduit

Let s be the electrical conductivity of the liquid, k the conductivity of the pipe wall, a and b the inner and outer radii of the pipe, respectively, and t the contact resistance per unit area between pipe wall and liquid, as shown in **Fig. 2**. Now the equations to be solved are as follows, where U_f and U_w denote the potential in the liquid and the wall, respectively:

$$\Delta U_f = B \frac{\partial V}{\partial y} \tag{9}$$

$$\Delta U_w = 0 \tag{10}$$

The boundary conditions for these equations are given at the inner and outer wall of the pipe:

At the inner surface of pipe wall, $r = a$,

$$s\frac{\partial U_f}{\partial r} = k\frac{\partial U_w}{\partial r}\ ;\ U_f + st\frac{\partial U_f}{\partial r} = U_w \tag{11}$$

And at the outer surface of pipe wall, $r = b$,

$$\frac{\partial U_w}{\partial r} = 0 \tag{12}$$

The first condition of equation (11) means the continuity of current, while the second one means the continuity of potential at the boundary.

The potential difference between the electrodes, which means the flowmeter output voltage, is obtained from the solution of equations (9) and (10) as shown in equation (13):

$$U_{fP} - U_{fQ} = 2Ba\nabla \frac{1+kt(b^2-a^2)/a(a^2+b^2)}{1+(k/s)(1+st/a)(b^2-a^2)/(a^2+b^2)} \quad (13)$$

We can assume that the conductivity of the metallic wall is much higher than the liquid conductivity and that it is also higher than the inverse of contact resistance:

$$k \gg s, \quad k \gg a/t \quad (14)$$

then equation (13) can be reduced to a simple expression (15):

$$U_{fP} - U_{fQ} = 2Ba\nabla \frac{st/a}{1+st/a} \quad (15)$$

The last factor of equation (15) describes how the flowmeter output is influenced by electrical conductivity. We can deduce following conclusions from equation (15):

(1) The output is influenced by liquid conductivity and contact resistance, but not by wall conductivity if it is much higher than that of the liquid.

(2) One of the important features of magnetic flowmeters would be lost, because the output is strongly dependent on the conductivity of liquid.

(3) If either or both of the liquid conductivity s or the contact resistance t is high enough, equation (15) approaches to the one for conventional magnetic flowmeters: $U_{fP} - U_{fQ} = 2Ba\nabla$.

(4) The larger the pipe radius a is, the more output is influenced by liquid conductivity s.

2.3 Effect of wall potential distribution

The idea is, if we control the potential at the inner surface of the wall to the same potential as given by equation (6), then the last result of equation (8) sets up a new boundary condition to compensate the effect of pipe conductivity.

Since, $U_w = U_f$, at $r = a$, equation (11) gives:

$$\frac{\partial U_f}{\partial r} = 0, \text{ at } r = a \quad (16)$$

The new boundary condition is clearly the same as that of the non-conducting wall, as given in equation (3), and it means that no current flows across the boundary, as long as the new boundary condition is satisfied.

If t increases to infinity in equation (15), then the flowmeter output, $U_{fP} - U_{fQ}$, approaches to $2Ba\nabla$, which is the output of a magnetic flowmeter having a pipe wall with non-conducting lining. This is the working principle of the proposed magnetic flowmeter. We call this new control method as the "potential compensation."

3 Electronic Circuits and Working Principles

3.1 Flowmetering system

A block diagram of experimental setup of new magnetic flowmeter is shown in **Fig. 3**.

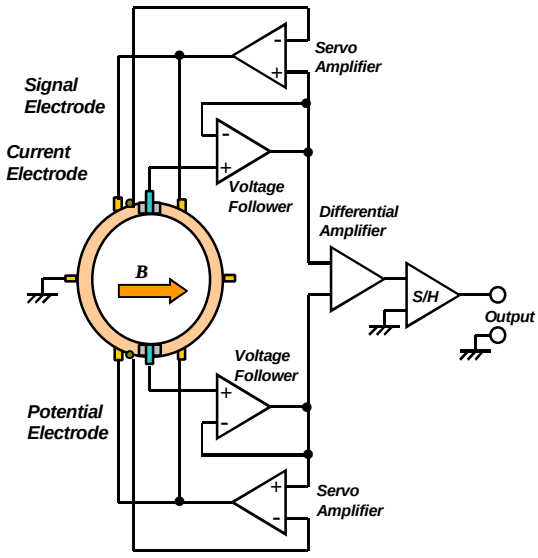

Fig. 3 Block diagram of the new magnetic flowmeter

The applied magnetic field is a square wave having a constant frequency of 3.125Hz.

The input impedance of amplifier first stage must be high enough. Otherwise, loading effect might cause an error and the compensation would not be perfect. Since the lower limit of liquid conductivity is usually about 5 ~ 10 μS/cm for magnetic flowmeters, the impedance between electrodes can be estimated at 500~1000kΩ, assuming the impedance is $1/sd$, where d is the electrode diameter and we assume $d = 2mm$. Input impedance of over $10^{10}\Omega$ is necessary to make the loading effect less than 0.01%. A voltage follower circuit using FET-input operational amplifiers is used at the first stage for this purpose.

The electronic circuit, which drives pipe wall potential for compensation, is a pair of servo amplifiers as shown in **Fig. 3**.

Other parts of electronics are almost identical to those of conventional magnetic flowmeters with low frequency square wave excitation of magnetic field. The flow signal is also square-wave, the signal output of the differential amplifier is sampled at the end of a positive and a negative half-cycle, respectively. The difference between these two sampled signals gives peak-to-peak value of output voltage, which is expected proportional to the flowrate. This configuration improves the immunity from noise, especially hum and quadrature components.

Fig. 4 shows a circuit of the servo amplifier. Because the conductivity of metal pipe wall is high, a high current gain is necessary for a servo amplifier.

3.2 Configuration of electrode of the flow pipe

Let us describe the structure of the flow transmitter of experimental model of the new magnetic flowmeter.

The flow pipe of stainless steel has 30mm outer

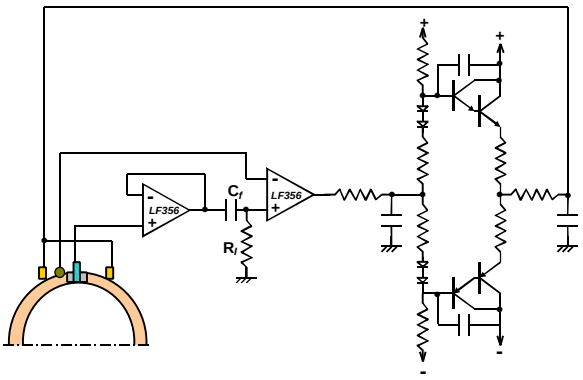

Fig. 4 The circuit of servo amplifier

diameter and 27mm inner diameter, and has a pair of electrodes, which are insulated from the pipe wall.

The flow transmitter is equipped of three different types of electrodes; signal electrodes (SE), current electrodes (CE), and potential electrodes (PE) – as shown in **Fig. 5**.

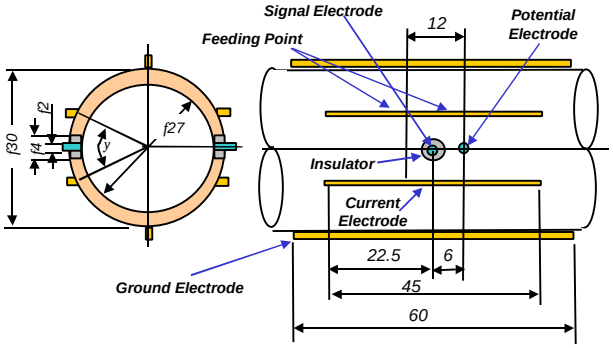

Fig. 5 Configuration of flow pipe and electrodes

A pair of the signal electrodes is insulated from the pipe as conventional transmitters. Diameter of the signal electrode is 2*mm*, which can be considered as a point if compared with pipe inner diameter. Diameter of insulator ring around signal electrode is 4 *mm*, this size has some effect on the signal level, when the compensation is not applied. However, the effect becomes negligible, when the compensation is applied.

A pair of separate potential electrodes is also welded to the outer pipe wall.

The current electrodes consisting of plates are welded near the signal electrodes.

Through the current electrodes, the servo amplifier feeds current to the pipe wall so as to make the voltage of PE same as that of SE, irrespective of potential drop due to the resistance of the welded junctions of CE and the lead wire. The location of the current electrodes is carefully positioned as point symmetry to SE.

Fig. 4 shows how the servo amplifier works in forming the potential distribution. The signal voltage detected by SE is applied to the input of the servo amplifier via voltage follower, and the voltage of PE is applied to another input of the servo amplifier as a feedback signal. The gain of servo amplifier is so high that the potential of PE is kept equal to the potential of SE.

The signal level of the experimental model is low, order of 10^{-4}V, and magnitude of feeding current is 1A at largest. Therefore the power consumption at pipe wall is less than 1 mW.

Thus angular distribution of potential on the pipe wall is trapezoidal, which is not completely compensation of sinusoidal one but a good approximation as shown in equation (6). The two corners on the trapezoid correspond to the angular locations of CE.

Let us discuss the longitudinal size of formed potential. The length of current electrode is 45*mm*, but the distance between upstream and downstream current feeding point is 12*mm*. Outside of this range, more than 1% reduction of magnetic field is observed.

4 Experimental Results and Discussion

4.1 Compensation effect of potential distribution

Test results are shown in **Figs 6** thru **10**. Theoretical values are shown by dotted line for reference in the figures.

(1) **Fig. 6** shows the correlation of the mean flowrate and output voltage using tap water (with conductivity s = 163 μS/cm). Without applied wall potential, the output is reduced down to about 60% of theoretical value

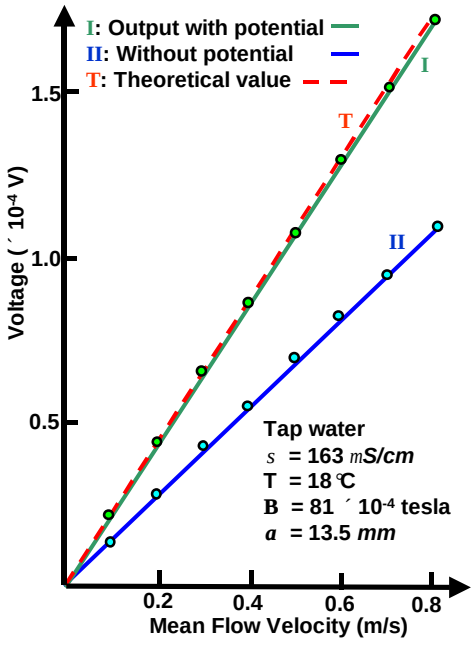

Fig. 6 Output Voltage vs. mean velocity

(solid line II); however, it can be increased to 99% of theoretical value with wall potential applied (solid line I).

(2) **Fig. 7** shows the effect of fluid conductivity *s*.

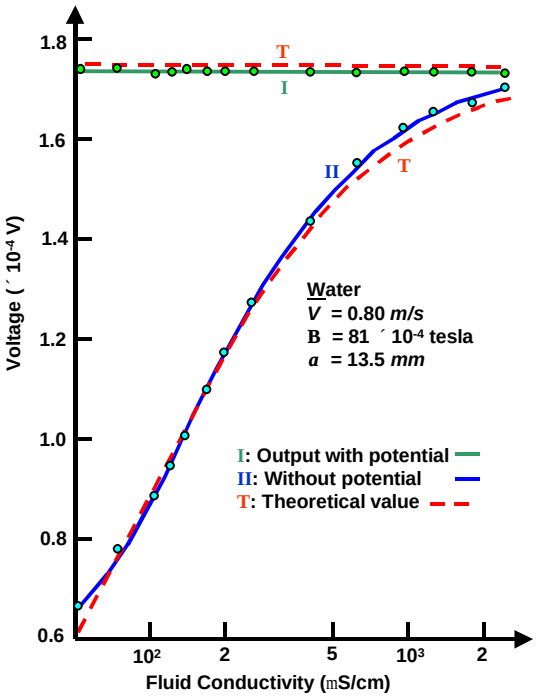

Fig. 7 Output voltage vs. fluid conductivity at constant flow rate

Equation (15) indicates that the flowmeter output is dependent on liquid conductivity without wall potential. Theoretical values are again shown by two dotted lines. The upper one indicates the theoretical value, when the pipe wall is non-conductive. The lower curve is calculated from equation (15). The contact resistance is assumed constant (t = 1.397 Ωm^2) and this value is calculated from the observed output at the conductivity of tap water (200 μS/cm), because of the technical difficulty in direct measurement of this quantity. Measured data are very close to the theoretical value, and large conductivity effect is observed without wall potential. However, no effect of liquid conductivity is observed if the wall potential is applied. The results suggest that the formed wall potential distribution is very effective, although the shape of distribution is an approximated one. Our assumption of constant t is correct.

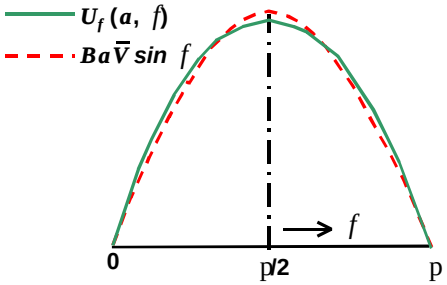

Fig. 8 Angular distribution of potential $U_f(a, f)$

(3) For comparison purpose, we measured the output of magnetic flowmeter having non-conducting tube of the same dimension, and the same magnetic field.

Obtained results are as follows:

- $U_1 = 1.76 \times 10^{-4}$ V, with a non-conducting pipe,
- $U_2 = 1.74 \times 10^{-4}$ V, with a compensated metal pipe,
- $U_3 = 1.75 \times 10^{-4}$ V, as calculated from equation (8),

In case of mean flow velocity = 0.8m/s, $B = 81 \times 10^{-4}$ *T*.

A uniform magnetic field along the pipe axis is assumed in calculating U_3, while the domain of uniform field is limited for experimental models.

Considering above assumptions, both U_1 and U_2 coincide well with calculated U_3.

4.2 Shape and magnitude of angular potential distribution

(1) **Fig. 8** shows theoretical and measured potential distribution, U_f (a, f). Angular distribution of the flow-induced potential is measured at the wall and liquid boundary. Keeping flow velocity constant at 0.8m/s, wall potential is measured for angle f = 0 to 90°, utilizing a pair of electrodes which is installed on the inner surface of non-conductive pipe wall.

. The cause of the small discrepancy can be regarded as following two reasons:

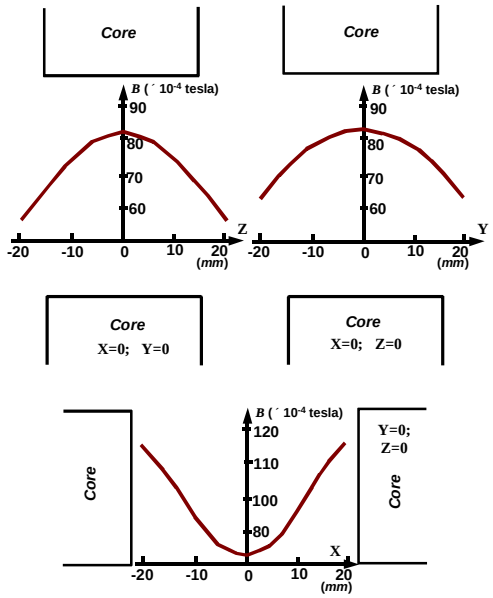

Fig. 9 Magnetic flux density distribution

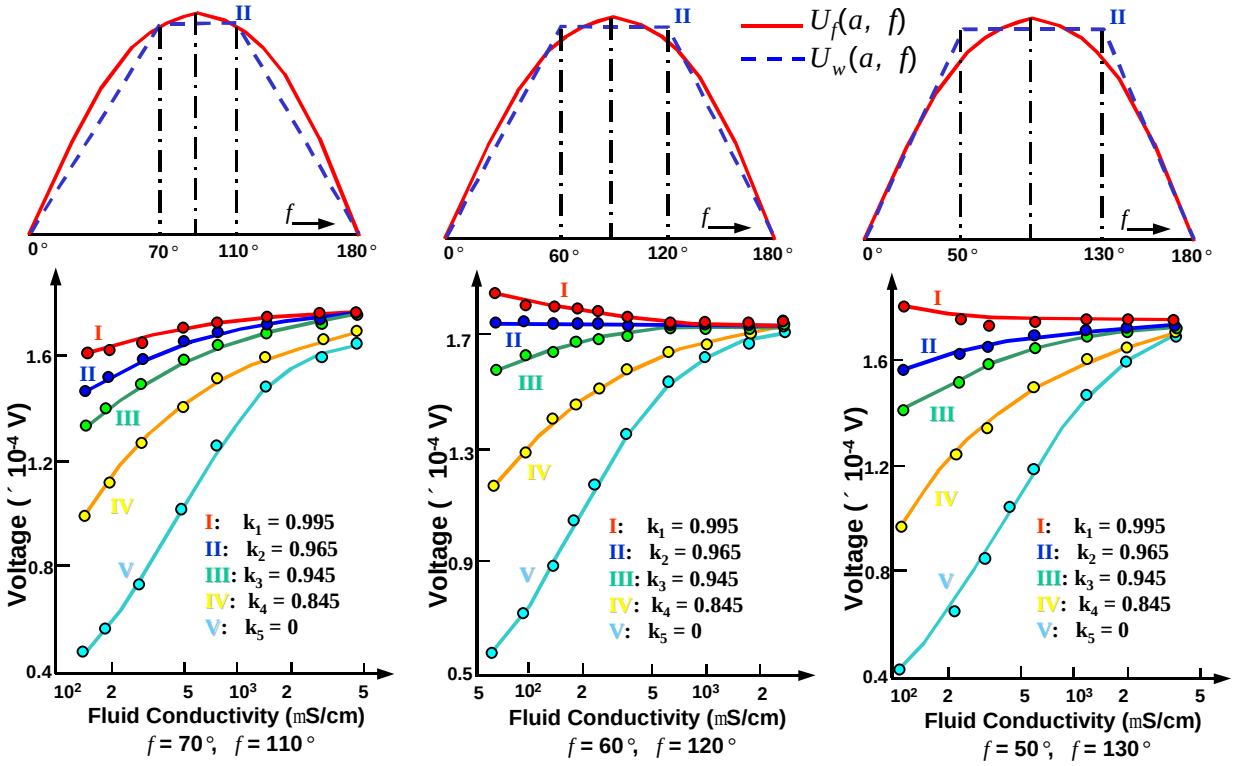

Fig. 10 Angular distribution of potential U_f and U_w, and output voltage vs. conductivity

a) Non-uniformity of the magnetic field

b) the finite size of electrodes

Measured magnetic flux density and spatial distribution are shown in **Fig. 9**. Along the X-axis, flux density increases near the pipe wall, and along the Y-axis, it decreases near the wall. The cause of the difference between theoretical and measured values of U_f at $f = p/2$ is regarded as the non-uniformity of flux density.

(2) **Fig. 10** shows the compensated potential and flowmeter output recovery. As discussed in 2.3, compensation potential distribution must be identical to that of the flow-induced potential, however, realized distribution is trapezoidal approximation as shown in **Fig. 8**. The characteristics of the new magnetic flowmeter are very dependent on the shape of potential distribution.

In order to find an optimum approximation, trial tests were made of three transmitters with different locations of current electrodes at various potential dividing ratios. Here the potential dividing ratio is defined as $k = U_{w\,max}/U_{f\,max}$.

The value of k can be changed by adjusting the resistor R_1 in the servo amplifier (see **Fig. 4**).

Using **Fig. 10**, the performance of test models is evaluated by the dependency of output for variation in the liquid conductivity s. The least dependency is the best. In the figures, f indicates the location of CE, and values of k are shown as parameters k_1, k_2, …, k_5 ($k_5 = 0$ means no potential distribution).

The experimental results can be summarized as follows:

a) The results suggest that there is an optimum combination of f and k; that is $f = 60°$ and $120°$, and $k = 0.965$. The flowmeter output is stable and not influenced for wide variation of liquid conductivity. The potential compensation works effectively although its angular distribution is a trapezoidal approximation of sinusoidal one.

b) In the case of $f = 70°$ and $110°$ (e.g., $y = 40°$), the compensation is not sufficient even for the highest $k = 0.995$. The output is reduced by lower conductivity. The reason is, $U_w(a, f)$ is lower than $U_f(a, f)$ outside of current electrodes ($f < 70°$ and $f > 110°$).

c) In the case of $f = 50°$ and $130°$ (e.g., $y = 80°$), the compensation is not sufficient if the optimum k is less than 0.9. If the k is bigger than 0.9, the feedback circuit becomes unstable. The feedback system is oscillatory for lower conductivity s.

d) Three different stainless pipes are used to install current electrodes in three different locations. They have a common diameter but different surface roughness and surface color, therefore, their contact resistance t of inner surface are different; 1.397 Ωm^2, 1.327 Ωm^2, 0.367 Ωm^2, respectively. Their outputs characteristics are very different when the potential

compensation is not applied. However, they are less sensitive on s when the potential compensation is applied.

5 Conclusions

In conclusion, on the basis of theoretical analysis and experimental data, the results of this investigation can be summarized as follows:

(1) A boundary condition, which is equivalent to that of a non-conducting pipe wall, can be achieved by applying voltage to the conductive pipe wall of a magnetic flowmeter.

(2) A proposed structure of magnetic flowmeter, having metallic pipe wall with the equivalent boundary condition, is realized by the use of electronic servo techniques.

(3) Experimental results agree well with calculated data based on the theoretical analysis.

(4) The optimum design parameters have been obtained and confirmed by experiments.

(5) One can expect the reliability and applicability of magnetic flowmeters to be improved by removal of the insulating liner.

Acknowledgement

The authors wish to express their gratitude to Mr. K. Asano and Mr. M. Okutomi for their effort for the feasibility study of this investigation.

References

1) H. Yamasaki et al.: Magnetic flowmeter having conducting pipe wall, 20th SICE Annual Meeting, Sendai, Japan, 1705 (1981)

2) H. Yamasaki et al.: Magnetic flowmeter having conducting pipe wall (Part 2), 21st SICE Annual Meeting, Tokyo, Japan, 3902 (1982)

3) K. Asano and M. Okutomi: Research on magnetic flowmeter, Graduation theses of The University of Tokyo (1981)

4) J.A. Shercliff: The theory of electromagnetic flow measurement, Cambridge Univ Press, 10/47.(1962)

5) M. Kawata, K. Komiya and H. Yamasaki as Editors: Handbook of flow measurement, Nikkan Kogyo Shinbunsha, Tokyo 275/276 (1979)

6) H. Yamasaki et al.: A Magnetic flowmeter with conducting pipe wall for expanded field of applications, Measurement Vol.2, No3,149/155 IMEKO (1984)

Hiro YAMASAKI (Member)

He received BE and Dr.E in applied physics from the University of Tokyo in 1956 and 1972 respectively. He worked for Yokogawa Electric Works from 1956 to 1974. He was a Professor in the University of Tokyo from 1975 to 1993. He worked for Yokogawa Electric Corp. as a Senior Vice President until 1995 and Yokogawa Research Institute Corp. as the Chairman of the Board until 2000. He was a President of SICE from 1989 to 1990. He is a professor emeritus of the University of Tokyo, Fellow of SICE and IEEE. His research interest is sensing technology and signal processing.

Satoshi HONDA (Member)

He graduated University of Tokyo in 1975 and received a PhD degree in 1985. He was an assistant professor (1975-1985) and a lecturer (1986) in University of Tokyo, an associate professor in Kumamoto University (1986-1990), and an associate professor (1990-1998) and a professor (1998-present) in Keio University. His current research interests are inverse problems in measurement physics. He is a member of SICE, Japanese society for medical and biological engineering, Japan society for industrial and applied mathematics, etc.

Dongzhi Jin (Member)

He graduated Industrial Automation Course in Huadong Institute of Chemical Industry in Shanghai, China in 1964 and received an M.S. degree from University of Tokyo in 1985, before joining Furukawa Electric Co,.Ltd. His interest is in sensor technologies for industrial application.

Chuji Akiyama (Member)

He graduated Nagoya University in 1974 and received an M.S. degree from University of Tokyo in 1976, before joining Yokogawa Electric Corporation. His interests are in sensors, control and industrial communication. He has been a member of ISA SP50 committee since 1981.

Reprinted/Translated from Trans. of the society of Instrumentation and Control Engineers Vol.19, No.5, 394/399 (1983)